Manuscript submitted to
AIMS' Journals
Volume **X**, Number **0X**, XX **200X**

doi:10.3934/xx.xx.xx.xx

pp. **X–XX**

POLARIZATION DYNAMICS IN A RESONANT OPTICAL MEDIUM WITH INITIAL COHERENCE BETWEEN DEGENERATE STATES

Abstract. We investigate the polarization switching phenomenon for a one-soliton solution to the Λ-configuration Maxwell-Bloch equations in the case of initial coherence in the material, corresponding to the forbidden transition between the two lower energy levels. We find two polarization states that are stationary. They are not the purely right- and left-circularly polarized solitons, as in the case of zero initial coherence, but rather two mixed, elliptically polarized, states. These polarization states, of which only one is asymptotically stable, depend on both the initial population levels of the lower states and the coherence value. We also find the existence of superluminal soliton propagation, but through numerical simulations show this solution to be unstable, and therefore likely not realizable physically.

Katherine A. Newhall*

University of North Carolina at Chapel Hill
Chapel Hill, NC 27599-3250, USA

Gregor Kovačič

Rensselaer Polytechnic Institute
Troy, NY 12180, USA

Ildar Gabitov

University of Arizona
Tucson, AZ 85721-0089, USA

(Communicated by the associate editor name)

1. **Introduction.** The resonant interaction between light and an active optical medium provides the basic mechanism underlying devices from lasers to optical amplifiers [1–4]. Depending on the structure of the atomic transitions, light is prepared to consist of one or more colors concentrated in narrow wavelength bands that interact with the specific electron transitions induced in the atoms composing the active medium [2,4]. Taking into account only the active atomic transitions, the description of the medium is given by the well-known Maxwell-Bloch equations [5–8]. For the most common situation, when the number of photons is large, the electric field envelope is described by classical dynamics while the material requires a quantum description, leading to a semi-classical system of equations [5].

2010 *Mathematics Subject Classification.* 78A40, 78A60, 78M35.

Key words and phrases. Maxwell-Bloch Equations, Dressing Method, Solitons, Polarization Switching.

The second author is supported by National Science Foundation (NSF) grant number DMS1615859.

* Corresponding author: xxxx.

The simplest resonant interaction takes place between monochromatic light and a transition between two working atomic levels [5]. The next simplest interaction involves light interacting with transitions among three working atomic levels, and often only with a pair of such transitions while the third transition is forbidden due to a selection rule [6–8]. The light involved in such an interaction may consist of a pair of colors, or else it may be monochromatic but consist of two polarizations. In this second case, the two transitions with equal strengths occur either between a degenerate, isoenergetic pair of lower-energy levels and an excited level, called the Λ-configuration medium, or one lower-energy level and two excited levels, called the V-configuration medium [6–8]. The Maxwell-Bloch system describing pulse interactions with either two-level atoms or two-level atoms with degeneracy is completely integrable when the relaxation times of the medium are long compared to the pulse width [5, 8, 9].

In the Λ-configuration, when all initial polarizations of the material are zero, there is a controllable switching phenomenon, described by a single soliton solution [10, 11]. Asymptotically at $t \to \pm\infty$, the solitary wave like solution approaches either purely left- or right-circular polarization with the alternate circular polarization component vanishing exponentially. If either circular polarization component is identically zero, then the pure circular polarization state is preserved, and no switching occurs. The existence of these two behaviors, switching and preserving polarization, allows for a control mechanism: for the unstable one of these circular polarizations, a small control pulse of the opposite polarization will induce switching of the polarization to the control pulse's polarization; the control pulse's polarization is stable. Which of the two circular polarizations is stable depends on the initial population of the lower energy levels in the material.

In this paper, we consider the case when the purely left- or right-circular polarization pulse switches to a mixed-polarization state of these two polarizations. This phenomenon is possible in the presence of initial coherence in the material, corresponding to the forbidden transition between the two lower levels. We find two polarization states that are preserved, however they are no longer the purely right- and left-circularly polarized solitons, but rather two mixed, elliptically polarized, states. Their eccentricity depends on both the initial population levels of the lower states and the initial coherence value. We describe this phenomenon in the framework of the integrable Maxwell-Bloch equations using the slowly-varying envelope and rotating-wave approximations [12–15].

The remainder of the paper is organized as follows. We present the Maxwell-Bloch equations that describe a Λ-configuration medium in Section 2. In Section 3, we outline the algebraic dressing method employed to obtain a single-soliton solution to the Maxwell-Bloch equations. Along with both electric field envelopes, we obtain equations describing the material polarizations and the atomic level occupations. Details of the method are found in the Appendix. We discuss the polarization-switching phenomenon in Section 4. Conclusions are presented in Section 5.

2. **The Maxwell-Bloch Equations.**

We model light interacting with a medium doped with three-level atoms. The lower energy state is degenerate, while the higher state is not, i.e. the medium is in the Λ configuration. Under the slowly-varying-envelope approximation for the electric field and medium polarization, the system is described by the quasi-classical Maxwell-Bloch equations [8, 11]. Under the additional approximation of an infinitely narrow spectral line of the electron

transitions under investigation, in the reference frame traveling at the speed of light, these equations are

$$\begin{aligned}
\partial_x E_\pm &= \rho_\pm && \text{(1a)}\\
\partial_t \rho_+ &= \tfrac{1}{2}\left[E_+(\mathcal{N}-n_+) - E_-\mu^*\right], && \text{(1b)}\\
\partial_t \rho_- &= \tfrac{1}{2}\left[E_-(\mathcal{N}-n_-) - E_+\mu\right], && \text{(1c)}\\
\partial_t \mathcal{N} &= -\tfrac{1}{2}\left[E_+{\rho_+}^* + {E_+}^*\rho_+\right] - \tfrac{1}{2}\left[E_-{\rho_-}^* + {E_-}^*\rho_-\right], && \text{(1d)}\\
\partial_t n_\pm &= \tfrac{1}{2}\left[E_\pm{\rho_\pm}^* + {E_\pm}^*\rho_\pm\right], && \text{(1e)}\\
\partial_t \mu &= \tfrac{1}{2}\left[{E_+}^*\rho_- + E_-{\rho_+}^*\right], && \text{(1f)}
\end{aligned}$$

where $*$ denotes the complex conjugate. In the above equations, the envelope of the electric field $E_+(x,t)$ corresponds to purely left-circularly polarized light, that takes part in the transitions between the lower sub-level population $n_+(x,t)$ and the excited-level population $N(x,t)$. The corresponding medium-polarization is $\rho_+(x,t)$. Similarly, the electric field envelope $E_-(x,t)$ for right-circularly polarized light takes part in the transition between $n_-(x,t)$ and $N(x,t)$ with corresponding medium-polarization $\rho_-(x,t)$. The coherence $\mu(x,t)$ corresponds to the forbidden transition between the two lower sub-level populations.

The initial conditions for (1) are set at $t \to -\infty$, well before the pulse of interest enters into the material. We take $E_\pm$ and $\rho_\pm$ to be zero initially, and consistently with the conserved quantity $n_+ + n_- + \mathcal{N} = 1$, we populate n_+ to $(1+\alpha)/2$ and n_- to $(1-\alpha)/2$ for some $\alpha \in [-1,1]$ and keep the excited state empty, $\mathcal{N}$=0. The boundary conditions for E_+ and E_- characterize the pulse that is sent into the material. We are interested in the propagation of a single soliton when initially there is a non-zero value μ_0 for the virtual polarization characterizing the coherence.

3. **The Single Soliton Solution.** Although the system in (1) is non-linear, it is in fact completely integrable. This is because this system can be written as a Lax Pair [9, 12–16]

$$\begin{aligned}
\partial_t \Psi &= U\Psi = i(\lambda J + H)\Psi, && \text{(2a)}\\
\partial_x \Psi &= V\Psi = -\frac{i}{4\lambda}\hat{\rho}\Psi, && \text{(2b)}
\end{aligned}$$

where

$$H = \frac{i}{2}\begin{pmatrix} 0 & E_+ & E_- \\ -E_+^* & 0 & 0 \\ -E_-^* & 0 & 0 \end{pmatrix}, \qquad \hat{\rho} = \begin{pmatrix} N & \rho_+ & \rho_- \\ \rho_+^* & n_+ & \mu \\ \rho_-^* & \mu^* & n_- \end{pmatrix},$$

$$J = \begin{pmatrix} 1 & 0 & 0 \\ 0 & -1 & 0 \\ 0 & 0 & -1 \end{pmatrix}.$$

The compatibility condition $\partial_x(\partial_t\Psi) = \partial_t(\partial_x\Psi)$ and collecting equations at the same order of the spectral parameter λ return the system (1).

Rather than apply the inverse scattering transform [17] to obtain soliton solutions to (2) as in [18] for the two level atom and [11, 19] for the Λ configuration, we use the simple algebraic dressing method [20], (see for example [21] for the two level atom or [22] for two different frequencies in the three level atom). The method is summarized here, with more details appearing in Appendix A. The general idea is to form the full solution for U and V at any position along x from a known solution

Ψ_0 corresponding to a stationary solution of the system. Then, when constructing the solution, the algebraic behavior of Ψ is fixed with respect to λ.

The stationary solution is found from the trivial problem with the coefficients U and V frozen at their initial values as $t \to -\infty$,

$$\begin{aligned} \partial_t \Psi_0 &= U_0 \Psi_0, \\ \partial_x \Psi_0 &= V_0 \Psi_0, \end{aligned} \tag{3}$$

where $U_0 = i\lambda J$ and $V_0 = -i\rho_0/4\lambda$ with

$$\rho_0 = \begin{pmatrix} 0 & 0 & 0 \\ 0 & \frac{1+\alpha}{2} & \mu_0 \\ 0 & \mu_0 & \frac{1-\alpha}{2} \end{pmatrix}, \tag{4}$$

in accordance with the initial conditions described in the last paragraph of the previous section. The solution to the constant coefficient matrix equation in (3) is $\Psi_0 = \exp(i\lambda J t - \frac{i}{4\lambda}\rho_0 x)$. The full solution Ψ is given in terms of the dressing matrix χ as

$$\Psi = \chi \Psi_0.$$

For the one-soliton solution with eigenvalue λ_0, the analytic structure of the dressing matrix χ is such that it has a pole at λ_0 [20], specifically

$$\chi = 1 - \frac{\lambda_0 - \lambda_0^*}{\lambda - \lambda_0^*} P. \tag{5}$$

Using this form of χ and $\Psi = \chi\Psi_0$ in (2a), it can be shown that the projection matrix P is a constant multiple of the known solution Ψ_0, where P can be written in the form

$$P = \frac{\vec{n}\vec{n}^\dagger}{\vec{n}^\dagger \vec{n}} \tag{6}$$

and $\vec{n}^\dagger$ is the complex conjugate transpose of $\vec{n}$, with

$$\vec{n} = \exp\left(i\lambda J t - \frac{i}{4\lambda}\rho_o x\right) \begin{pmatrix} 1 \\ a \\ b \end{pmatrix} \tag{7}$$

for arbitrary complex constants a and b describing the proportion of the soliton in the E_+ and E_- polarized state, respectively.

Solving (2) for U and V in terms of the dressing matrix χ, and therefore in terms of the elements of the projection matrix P, we find that the electric field envelopes and elements of the density matrix are given by the equations

$$E_+(x,t) = -4i(\lambda_0 - \lambda_0^*)P_{12}, \tag{8a}$$
$$E_-(x,t) = -4i(\lambda_0 - \lambda_0^*)P_{13}, \tag{8b}$$
$$N(x,t) = -4i(\lambda_0 - \lambda_0^*)(\partial_x P)_{11}, \tag{8c}$$
$$n_+(x,t) = \frac{1+\alpha}{2} - 4i(\lambda_0 - \lambda_0^*)(\partial_x P)_{22}, \tag{8d}$$
$$n_-(x,t) = \frac{1-\alpha}{2} - 4i(\lambda_0 - \lambda_0^*)(\partial_x P)_{33}, \tag{8e}$$
$$\rho_+(x,t) = -4i(\lambda_0 - \lambda_0^*)(\partial_x P)_{12}, \tag{8f}$$
$$\rho_-(x,t) = -4i(\lambda_0 - \lambda_0^*)(\partial_x P)_{13}, \tag{8g}$$
$$\mu(x,t) = \mu_0 - 4i(\lambda_0 - \lambda_0^*)(\partial_x P)_{23}. \tag{8h}$$

Purely imaginary poles yield the simplest solitons, which have real-valued electric-field envelopes [9]. Therefore, to obtain such a single-soliton solution, we take $\lambda_0 = i\beta$, and define

$$\nu = \sqrt{\alpha^2 + 4\mu_0^2}\,, \tag{9}$$

finding that (8a) and (8b) reduce to (written in the lab frame rather than the light-cone frame traveling at speed $c = 1$)

$$E_+ = \frac{4\beta A^*}{\sqrt{|A|^2 + |B|^2}} \operatorname{sech}\Theta(x,t), \tag{10a}$$

$$E_- = \frac{4\beta B^*}{\sqrt{|A|^2 + |B|^2}} \operatorname{sech}\Theta(x,t), \tag{10b}$$

where

$$\Theta(x,t) = 2\beta(t-x) - \frac{(1+\nu)x}{8\beta} + \frac{1}{2}\ln\left(|A|^2 + |B|^2\right),$$

and

$$A = \tfrac{a\nu + a\alpha + 2b\mu_0}{2\nu} + e^{\nu x/4\beta}\left(\tfrac{a\nu - a\alpha - 2b\mu_0}{2\nu}\right), \tag{11a}$$

$$B = \tfrac{2a\mu_0 - b\alpha + b\nu}{2\nu} - e^{\nu x/4\beta}\left(\tfrac{2a\mu_0 - b\alpha - b\nu}{2\nu}\right). \tag{11b}$$

The imaginary part of λ_0, β, controls the width of the soliton pulse. For any μ_0, the parameters a and b control the polarization of the initial pulse at $x = 0$: $A(x=0) = a$ and $B(x=0) = b$ corresponding to the amplitudes of E_+ and E_- respectively. Notice that, when $\mu_0 \to 0$, we recover the one-soliton solution appearing in [11] since $\nu \to |\alpha|$ in this case.

Explicit expressions for the material properties contained within the density matrix can be obtained from (8c) to (8h), but are too unwieldy to be presented here. For the case when $\mu_0 = 0$, the exact expressions appear in Appendix B. We do present the material descriptors for non-zero μ_0 in the case of the asymptotically stable soliton below in (14).

4. **Dynamics of the Single Soliton Solution.** The electric fields in (10) describe the propagation of a soliton pulse as it interacts with the material described by Eqs. (8c) to (8h). The electric field solutions are used to demonstrate the polarization switching phenomenon explained in the introduction. The polarization switching phenomenon has been investigated in [11] in the absence of initial coherence between the sublevels ($\mu_0 = 0$) and in [23, 24] for the case of random initial populations in the lower two energy levels. These spatially disordered populations are modeled by allowing the population difference $\alpha = n_+ - n_-$ in the initial population matrix ρ_0 in (4) to be a random function of the distance into the material, x. In both these cases, the polarization-switching phenomenon is entirely controlled by the cumulative value of $\alpha(x)$ the pulse sees while traveling down the material. In particular, if $\int_0^x \alpha(z)dz \to \infty$ (on average for the case of random $\alpha(x)$) as the pulse propagates down the material, the polarization of the light pulse tends toward left-circularly polarized ($E_+ \to 0$). If $\int_0^x \alpha(z)dz \to -\infty$, then the polarization of the light pulse tends toward right-circularly polarized ($E_- \to 0$).

If the medium is prepared in such a way as to have an initial coherence between the sublevels, then there are striking differences with the above previously-known results. The circularly-polarized soliton pulse no longer remains invariant and the final polarization state depends explicitly on the values of α and μ_0. As shown

in Fig. 1, an initially circularly-polarized soliton switches to a mixed-polarization state rather than remaining unchanged as in the case of $\mu_0 = 0$. We obtain this asymptotically-stable mixed-polarization state by finding the asymptotic expressions for the electric fields in (10) and the material in Eqs. (8c) to (8h) deep into the material, i.e. as $x \to \infty$. There exists a second mixed-polarization state that remains unchanged when propagating through the material, but this state is unstable, and can therefore be found by looking at the asymptotic expression for the electric field as $x \to -\infty$. Furthermore, as demonstrated in Fig. 2, the material only returns to its initial state for a soliton pulse of these specific polarizations. The initial soliton pulse in Fig. 2, which is not one of these two asymptotic polarization states, leaves behind a higher n^+ population and lower n^- population than those that the material initially started with. This population change decreases down the length of the material as the soliton pulse approaches its asymptotic state. The material is only truly transparent to soliton pulses with either of the two asymptotic polarization states.

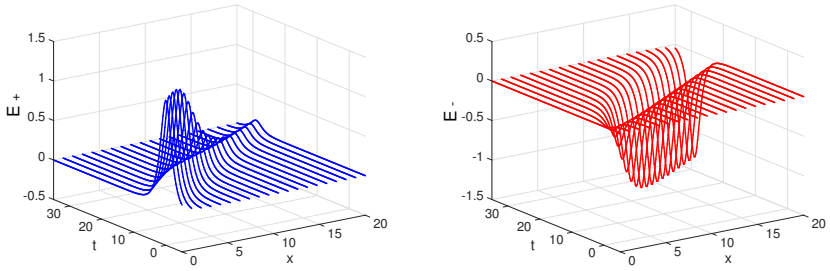

FIGURE 1. The solution to the Maxwell-Bloch equations appearing in (10), plotted in the lab frame of reference for an initially circularly-polarized soliton pulse ($a = 1$, $b = 0$, $\beta = 1/3$). With the virtual polarization initially $\mu_0 = 0.05$, and the initial population offset $\alpha = \frac{1}{2}$, the soliton switches its polarization to a mixed-polarization state.

4.1. **Asymptotic Behavior.** In this section, we present the asymptotic behavior of the single-soliton electric fields in both the $x \to +\infty$ and $x \to -\infty$ limits. For the asymptotically stable, $x \to \infty$ case, we also present expressions for the limiting behavior of the material properties, which emphasizes that the material remains unchanged after the soliton corresponding to the stationary polarization state passes through it.

For the electric fields given by (10), as $x \to \infty$, the amplitude of the soliton is dominated by the exponential terms in the expressions A and B given in (11), resulting in the electric fields being dominated by

$$E_+ \to \frac{4\beta A_\infty^*}{\sqrt{|A_\infty|^2 + |B_\infty|^2}} \operatorname{sech} \Theta_\infty(x,t), \qquad (x \to \infty), \tag{12a}$$

$$E_- \to \frac{4\beta B_\infty^*}{\sqrt{|A_\infty|^2 + |B_\infty|^2}} \operatorname{sech} \Theta_\infty(x,t), \qquad (x \to \infty), \tag{12b}$$

where

$$\Theta_\infty(x,t) = 2\beta(t-x) - \frac{(1-\nu)x}{8\beta} + \frac{1}{2}\ln\left(|A_\infty|^2 + |B_\infty|^2\right),$$

and the amplitudes are given by

$$A_\infty = \frac{1}{2\nu}(a\nu - a\alpha - 2b\mu_0), \tag{13a}$$

$$B_\infty = \frac{1}{2\nu}(-2a\mu_0 + b\alpha + b\nu), \tag{13b}$$

where $\nu = \sqrt{\alpha^2 + 4\mu_0^2}$ as defined in (9). Notice with $\mu_0 = 0$ the value of $\nu = |\alpha|$, and we have

$$A_\infty = 0, \quad B_\infty = 1, \quad \text{for } \alpha > 0,$$
$$A_\infty = 1, \quad B_\infty = 0, \quad \text{for } \alpha < 0,$$

corresponding to the purely right- and left-circularly polarized soliton respectively, as expected.

From the expressions for the material properties in Eqs. (8c) to (8h), we extract the dominant exponential terms as $x \to \infty$. The occupation of the energy levels and the virtual polarization are given by the expressions

$$N \to \frac{1-\nu}{2}\operatorname{sech}^2\Theta_\infty(x,t), \tag{14a}$$

$$n_+ \to \frac{1+\alpha}{2} - \frac{(1-\nu)}{2}\frac{S_+}{\nu T}\operatorname{sech}^2\Theta_\infty(x,t), \tag{14b}$$

$$n_- \to \frac{1-\alpha}{2} - \frac{(1-\nu)}{2}\frac{S_-}{\nu T}\operatorname{sech}^2\Theta_\infty(x,t), \tag{14c}$$

$$\mu \to \mu_0 + \frac{(1-\nu)}{2}\frac{\mu_0}{\nu}\operatorname{sech}^2\Theta_\infty(x,t), \tag{14d}$$

as $x \to \infty$, where we have defined

$$T = 2\nu(|A_\infty|^2 + |B_\infty|^2) = |a|^2(\nu-\alpha) - 2(ab^* + a^*b)\mu_0 + |b|^2(\nu+\alpha),$$
$$S_+ = |a|^2(\alpha^2 - \alpha\nu + 2\mu_0^2) + (\alpha-\nu)\mu_0(ab^* + a^*b) + 2\mu_0^2|b|^2,$$
$$S_- = |b|^2(\alpha^2 + \alpha\nu + 2\mu_0^2) - (\alpha+\nu)\mu_0(ab^* + a^*b) + 2\mu_0^2|a|^2.$$

Notice with $\mu_0 = 0$ we have

$$S_+ = 0, \quad \frac{S_-}{\nu T} = 1, \quad \text{for } \alpha > 0,$$
$$\frac{S_+}{\nu T} = 1, \quad S_- = 0, \quad \text{for } \alpha < 0,$$

and μ remains identically zero, corresponding to the transitions of purely right- and left-circularly polarized light respectively, as expected. The polarizations as $x \to \infty$ are given by

$$\rho_+ \to \frac{(1-\nu)}{2}\frac{R_1}{\nu T}\sqrt{\left|\frac{R_2}{R_1}\right|}\sinh\Theta_{21}(x,t)\operatorname{sech}^2\Theta_\infty(x,t) \tag{14e}$$

$$\rho_- \to \frac{(1-\nu)}{2}\frac{R_3}{\nu T}\sqrt{\left|\frac{R_4}{R_3}\right|}\sinh\Theta_{43}(x,t)\operatorname{sech}^2\Theta_\infty(x,t) \tag{14f}$$

where we have defined

$$\begin{aligned}
\Theta_{jk}(x,t) &= 2\beta(t-x) - \frac{(1-\nu)x}{8\beta} + \frac{1}{2}\ln\left|\frac{R_j}{R_k}\right|,\\
R_1 &= \nu(a^*(\nu-\alpha) - 2\mu_0 b^*),\\
R_2 &= (a^*)^2(-2a\mu_0^2 + (a\nu - b\mu_0)(\nu-\alpha))\\
&\quad - 2\mu_0 a^* b^*(a(\nu-\alpha) - 2\mu_0 b) + (b^*)^2\mu_0(2a\mu_0 - b(\nu+\alpha)),\\
R_3 &= \nu(b^*(\nu+\alpha) - 2\mu_0 a^*),\\
R_4 &= (a^*)^2\mu_0(-a(\nu-\alpha) + 2b\mu_0) - 2\mu_0 a^* b^*(-2a\mu_0 + b(\nu+\alpha))\\
&\quad + (b^*)^2((b\nu - a\mu_0)(\nu+\alpha) - 2b\mu_0^2).
\end{aligned}$$

To find the second, unstable, stationary polarization state we take $x \to -\infty$. In this case, the electric fields given by (10) are dominated by the sub-exponential terms in the expressions A and B given in (11). The soliton has the form,

$$E_+ \to \frac{4\beta A^*_{-\infty}}{\sqrt{|A_{-\infty}|^2 + |B_{-\infty}|^2}}\operatorname{sech}\Theta_{-\infty}(x,t) \quad (x \to -\infty), \tag{15a}$$

$$E_- \to \frac{4\beta B^*_{-\infty}}{\sqrt{|A_{-\infty}|^2 + |B_{-\infty}|^2}}\operatorname{sech}\Theta_{-\infty}(x,t) \quad (x \to -\infty), \tag{15b}$$

with

$$\Theta_{-\infty}(x,t) = 2\beta(t-x) - \frac{(1+\nu)x}{8\beta} + \frac{1}{2}\ln\left(|A_{-\infty}|^2 + |B_{-\infty}|^2\right),$$

and amplitudes given by

$$A_{-\infty} = \frac{1}{2\nu}(a\nu + a\alpha + 2b\mu_0), \tag{16a}$$

$$B_{-\infty} = \frac{1}{2\nu}(2a\mu_0 - b\alpha + b\nu). \tag{16b}$$

4.2. **Polarization Characterization.** In order to describe the mixed-polarization states that are stationary, we quantify the polarization ellipse that the electric fields map out in terms of two angles, η and ψ. The angle of ellipticity η, defined via the expression

$$\sin 2\eta = \frac{|E_+|^2 - |E_-|^2}{|E_+|^2 + |E_-|^2}, \tag{17}$$

is related to the ellipticity, the ratio of the semi-minor to the semi-major axis of the polarization ellipse. It ranges from left-circularly polarized at $\eta = -\pi/4$ through linearly polarized at $\eta = 0$ to right-circularly polarized at $\eta = \pi/4$. The polarization azimuth ψ, defined via the formula

$$\tan 2\psi = i\frac{E_+E_-^* - E_-E_+^*}{E_+E_-^* + E_-E_+^*}, \tag{18}$$

ranging from $-\pi/4$ to $\pi/4$, describes the orientation of the semi-major axis of the polarization ellipse. This orientation angle is defined relative to the constants a and b of the initial pulse at $x = 0$. It defines the y-axis so that the semi-major axis of the polarization ellipse at $x = 0$ and the y-axis make an angle ψ given by $\tan 2\psi = i\frac{ab^* - a^*b}{a^*b + ab^*}$. The semi-major axis at $x = 0$ is the y-axis if both a and b are real.

The polarization depends solely on the depth into the material to which the pulse has propagated, thus both $\eta(x)$ and $\psi(x)$ are functions of x only. The stationary

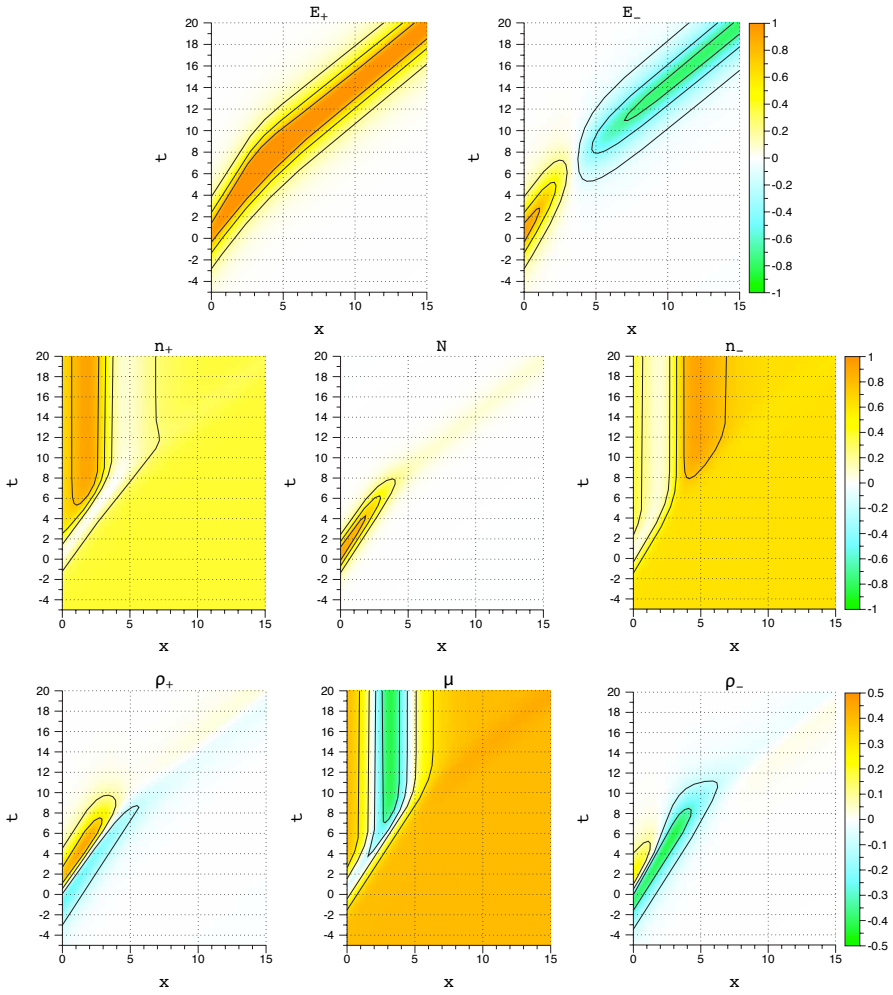

FIGURE 2. The solution to the Maxwell-Bloch equations appearing in (8) plotted in the lab frame of reference for an initially linearly-polarized soliton pulse ($a = 1/2$, $b = 1/2$, $\beta = 1/3$). The color bar is the same for each row. The other parameters are $\alpha = -0.25$, and $\mu_0 = 0.4$. The corresponding value of $\sin(2\eta)$ for this soliton as it propagates is shown in Fig. 3 (right).

polarizations are therefore determined solely by the two sets of limiting amplitudes of the electric fields given by (13) and (16). From (17), together with either (13) or (16), the eccentricity angles are given by the expressions

$$\sin 2\eta = -\frac{\alpha}{\nu} = \frac{-\alpha}{\sqrt{\alpha^2 + 4\mu_0^2}}, \tag{19}$$

$$\sin 2\eta = \frac{\alpha}{\nu} = \frac{\alpha}{\sqrt{\alpha^2 + 4\mu_0^2}}. \tag{20}$$

These two stationary polarizations describe the asymptotic polarization states of the electric fields. The first state (19), quantifies the stable polarization state; the

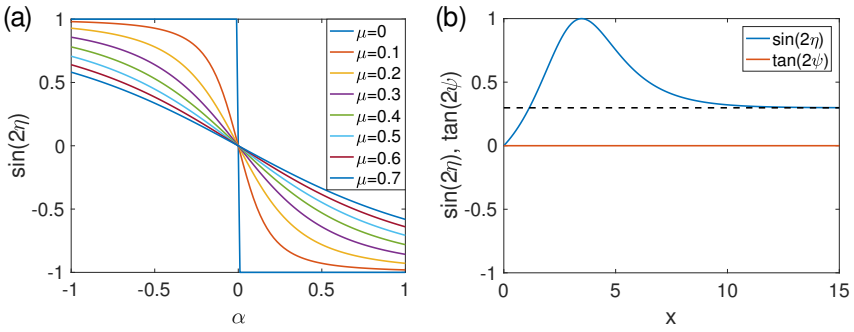

FIGURE 3. (a) The limiting value of $\sin(2\eta)$ for the stable invariant polarization state given by the expression in (19), as a function of α for the indicated values of μ_0 starting at 0 and increasing by 0.1 until $\mu_0 = 0.7$. (b) Dynamics of $\sin(2\eta)$ approaching its limiting value in (19) for the soliton depicted in Fig. 2, $\alpha = -0.25$, and $\mu_0 = 0.4$

dependence of $\sin 2\eta$ on μ_0 and α is shown in Fig. 3(a). The second asymptotic state, (20), quantifies the unstable polarization state; it is the reflection of the plot in Fig. 3(a). It describes the $x \to -\infty$ asymptotic of the polarization state of the electric fields. The stable state indeed reduces to the known $\mu_0 = 0$ case, (recall $\nu = |\alpha|$ when $\mu_0 = 0$),

$$\sin 2\eta = \begin{cases} 1 & \alpha < 0 \\ -1 & \alpha > 0 \end{cases} .$$

The stable polarization state in this case is either the right- or left-circular polarization, and depends only on which initial state, n_+ or n_-, is more populated. The unstable polarization state is the opposite circular polarization. Similarly, which of the states $\sin 2\eta = \pm|\alpha|/\nu$ is stable is determined by the sign of α when $\mu_0 \neq 0$; when $\alpha < 0$ the $+|\alpha|/\nu$ state is stable, while when $\alpha > 0$, the $-|\alpha|/\nu$ state is stable.

From (18), together with either (13) or (16), we find that the orientation angle of either the stable or unstable stationary polarization state is given by

$$\tan 2\psi = 0 \qquad \mu_0 \neq 0. \tag{21}$$

The case of $\mu_0 = 0$ is a degenerate case when both the numerator and denominator tends to zero. We recover the known stable stationary polarization, $\tan 2\psi = i\frac{ab^* - a^*b}{ab^* + a^*b}$, by taking the limit as $\mu_0 \to 0$. Note however that if the eigenvalue corresponding to the soliton solution is allowed to have a real part, introducing a phase to the soliton, then for the $\mu_0 = 0$ case the angle ψ is known to forever rotate. Returning to (8), we calculate the soliton propagation for an eigenvalue with real part and small, but non-zero $\mu_0 = 0.02$. As seen in Fig. 4, the angle ψ rotates a few times before approaching its asymptotic value of zero, in contrast to the $\mu_0 = 0$ case for which it forever rotates.

4.3. **Soliton Speed.** With non-zero initial coherence, we are able to find soliton solutions that travel faster than the speed of light. Such superluminal light pulses have been realized in physical systems, for example using gain-assisted linear anomalous dispersion in three-level atoms [25]. From (12) we see that the speed at which

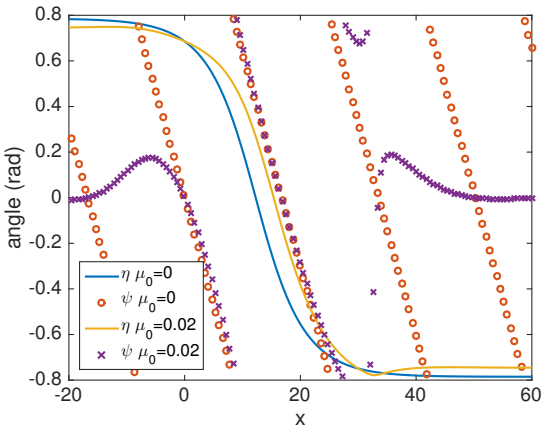

FIGURE 4. The dynamics of the angles η and ψ for the case of a soliton with the eigenvalue $\lambda_0 = \frac{1}{3} + \frac{1}{3}i$. Two cases are shown, one for $\mu_0 = 0$ and one for $\mu_0 = 0.02$ showing the difference between the behavior of the angle ψ. The other parameters are $a = 1$, $b = \frac{1}{10}$, and $\alpha = \frac{1}{2}$.

the long-time soliton travels is

$$u = \left[1 + \frac{1-\nu}{16\beta^2}\right]^{-1}. \tag{22}$$

where β is the imaginary part of the soliton eigenvalue, characterizing the shape of the pulse. For the case of $\mu_0 = 0$, the value of $\nu = |\alpha|$ and the soliton speed is always slower than the speed of light ($c = 1$), approaching it as $\alpha \to \pm 1$, corresponding to all initial populations in either n^+ or n_-. However, for values of

$$|\mu_0| > \sqrt{\frac{1-\alpha^2}{4}}$$

the value of $\nu > 1$ and the light pulse travels at a speed greater than 1. We show one such example in Fig. 5. Notice that the large value of μ_0 is allowing the state populations to become negative; it behaves as an additional population state. In reality, this type of solution would never be realized as it is unstable. The Darboux transformation used to construct the solution does not capture the continuous radiation shed by this unstable soliton. By integrating the Maxwell-Bloch equations in (1) numerically instead, we capture this shedding of radiation and see in Fig. 6 that the pulse is unstable and slows down to travel at the speed to light.

5. **Conclusions.** Through the use of the dressing method to obtain the one-soliton solution to the Λ-configuration Maxwell-Bloch equations, we investigated the polarization switching phenomenon in the case of non-zero initial coherence in the material, $\mu_0 \neq 0$. The material is completely transparent to two elliptically polarized soliton pulses, characterized by an eccentricity angle that depends on both μ_0 and the initial difference in ground population levels, α; only one is stable. This result can be used as a tool for identifying the initial coherence in the material. By measuring the eccentricity of a pulse as it exits a material, the coherence can be

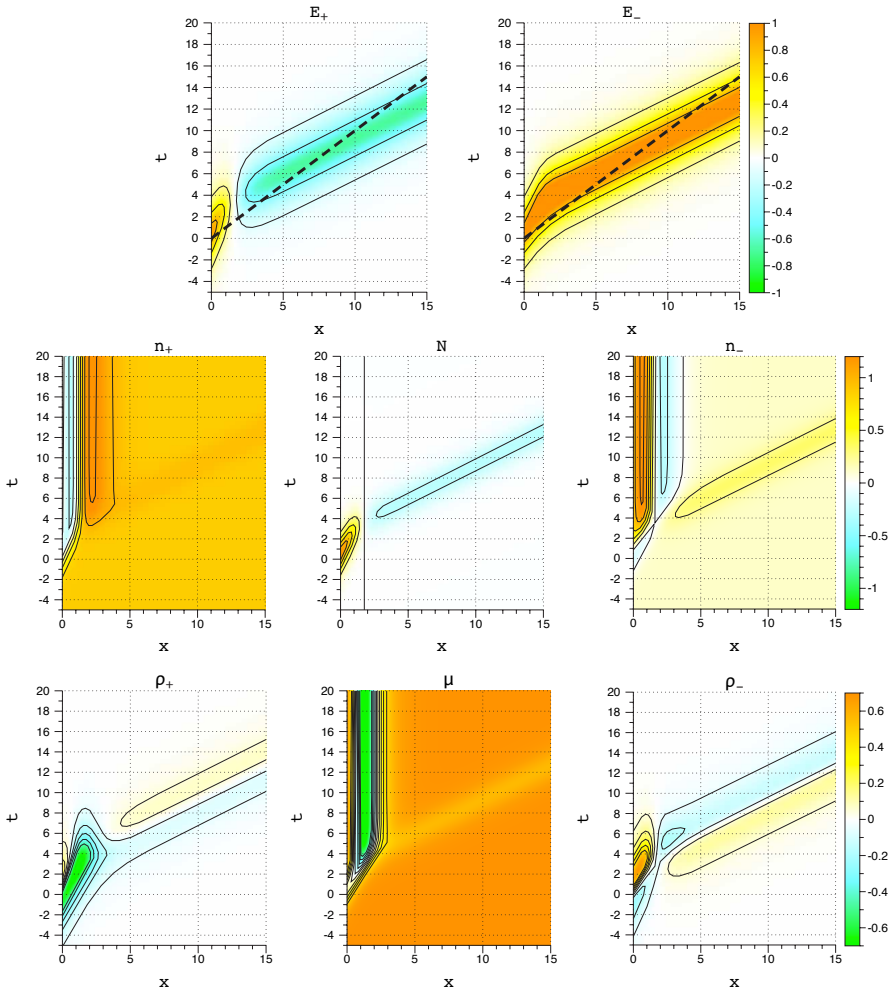

FIGURE 5. An unphysical solution to the Maxwell-Bloch equations appearing in (8) plotted in the lab frame of reference for an initially linearly polarized soliton pulse ($a = 1/2$, $b = 1/2$, $\beta = 1/3$). The color bar is the same for each row. The other parameters are $\alpha = 0.75$, and $\mu_0 = 0.7$. The dashed lines in the top row are drawn at the speed of light ($c = 1$) highlighting the fact that the soliton is propagating faster than the speed of light.

obtained from (19) if the initial populations of the material are known. We also showed the existence of a soliton traveling faster than the speed of light, which we expect to be unstable and therefore not realizable physically. The exact one-soliton solution does not permit for continuous radiation to be shed, which does occur in the numerically computed faster-than-light soliton solution.

Appendix A. Dressing Method. Step 1: write solution in terms of dressing matrix

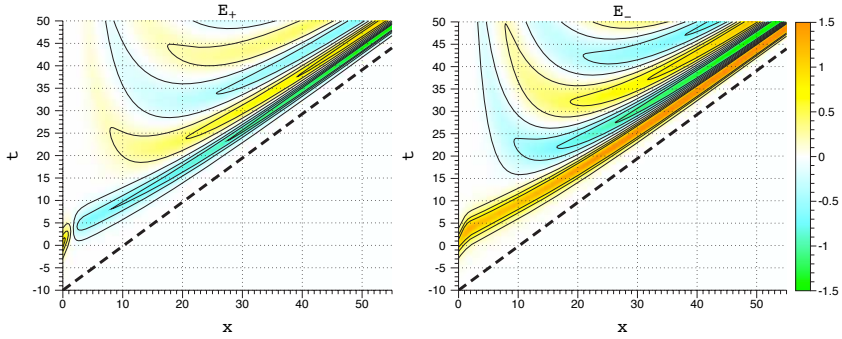

FIGURE 6. The electric-field envelopes computed by numerically solving the Maxwell-Bloch equations in (1) using the method described in Appendix C with $\Delta x = \Delta t = 0.05$. The faster-than-light soliton solution shown in Fig. 5 ($a = 1/2$, $b = 1/2$, $\beta = 1/3$, $\alpha = 0.75$, and $\mu_0 = 0.7$) is unstable and sheds radiation, slowing down to propagate at the speed of light (the dashed line).

With the ansatz that

$$\Psi = \chi \Psi_0,$$

with Ψ_0 solving the system (3), the Lax Pair equations in (2) become

$$\partial_t(\chi)\Psi_0 + \chi U_0 \Psi_0 = U \chi \Psi_0,$$
$$\partial_x(\chi)\Psi_0 + \chi V_0 \Psi_0 = V \chi \Psi_0.$$

Solving for U and V, we obtain

$$\begin{aligned} U &= \partial_t(\chi)\chi^{-1} + \chi U_0 \chi^{-1}, \\ V &= \partial_x(\chi)\chi^{-1} + \chi V_0 \chi^{-1}. \end{aligned} \tag{23}$$

Step 2: determine dressing matrix

This is to help determine the projection matrix P in (6). The equation for U in (23) can be rewritten as

$$U = \chi(U_0 - \partial_t)\chi^{-1} \tag{24}$$

by inserting $\chi\chi^{-1}$ before $\partial_t \chi$ and then noting that $\partial_t \chi^{-1} = -\chi^{-1}\partial_t(\chi)\chi^{-1}$. Then, inserting the form of χ from (5), we find

$$U = \left(1 - \frac{\lambda_0 - \lambda_0^*}{\lambda - \lambda_0^*} P\right)(U_0 - \partial_t)\left(1 - \frac{\lambda_0^* - \lambda_0}{\lambda - \lambda_0} P\right). \tag{25}$$

We know U describing the electric fields will have no poles, so the residue at $\lambda = \lambda_0$ of the right hand side must vanish, and so

$$[(1 - P)(U_0 - \partial_t)(\lambda_0 - \lambda_0^*)P]_{\lambda=\lambda_0} = 0. \tag{26}$$

Since $(1 - P)$ does not vanish (this would make the projection matrix trivial), we must have

$$[(U_0 - \partial_t)P]_{\lambda=\lambda_0} = 0,$$

or

$$[P_t]_{\lambda=\lambda_0} = [U_0 P]_{\lambda=\lambda_0},$$

and we see that P solves the same equation that Ψ_0 solves with $\lambda = \lambda_0$, and therefore must be a constant multiplier of this known solution. The known solution

Ψ_0 is trivial to find, as it solves the constant-coefficient equations in (3). It is given by

$$\Psi_0 = \exp\left(i(\lambda J + U_0)t - \frac{i}{4\lambda}\rho_0 x\right).$$

The projection matrix P is considered to project onto a line, and therefore has the form

$$P = \frac{\vec{n}\vec{n}^\dagger}{\vec{n}^\dagger\vec{n}} \tag{27}$$

where

$$\vec{n} = \exp\left(i(\lambda_0 J + U_0)t - \frac{i}{4\lambda}\rho_0 x\right)\begin{pmatrix}1\\ a\\ b\end{pmatrix} \tag{28}$$

where a and b are the complex constants describing the amount of the soliton solution that is initially in the E_+ and E_- channels, respectively.

Step 3: determine desired variables in terms of projection matrix

Starting from (25), we insert the expressions for U and U_0 to obtain

$$i(\lambda J + H) = \left(1 - \frac{\lambda_0 - \lambda_0^*}{\lambda - \lambda_0^*}P\right) i\lambda J \left(1 - \frac{\lambda_0^* - \lambda_0}{\lambda - \lambda_0}P\right)$$

and then expand for large λ, to find

$$i\lambda J + iH = i\lambda J - i(\lambda_0 - \lambda_0^*)PJ - i(\lambda_0^* - \lambda_0)JP + \dots,$$

where the dots contain terms with poles. Simplifying, we obtain $H = -(\lambda_0 - \lambda_0^*)[P, J]$ where $[\cdot,\cdot]$ is the matrix commutator. Extracting the appropriate components gives the expressions for E_+ and E_- in (8a) and (8b). Specifically, using the projection matrix P given in (27) with $\vec{n}$ given in (28), and simplifying, we arrive at the expressions for the two electric fields in (10).

For the density matrix, inserting in the expressions for V, V_0, and χ into (23) we find

$$\begin{aligned}\frac{i}{4\lambda}\hat{\rho} = &\left(1 - \frac{\lambda_0 - \lambda_0^*}{\lambda - \lambda_0^*}P\right)\left(\frac{i}{4\lambda}\rho_0\right)\left(1 - \frac{\lambda_0^* - \lambda_0}{\lambda - \lambda_0}P\right)\\ &+ \left(-\frac{\lambda_0 - \lambda_0^*}{\lambda - \lambda_0^*}\partial_x P\right)\left(1 - \frac{\lambda_0^* - \lambda_0}{\lambda - \lambda_0}P\right).\end{aligned}$$

Multiplying through by $-4i\lambda$ and expanding the second term for large λ, we compute

$$\begin{aligned}\hat{\rho} = &\left(1 - \frac{\lambda_0 - \lambda_0^*}{\lambda - \lambda_0^*}P\right)\rho_0\left(1 - \frac{\lambda_0^* - \lambda_0}{\lambda - \lambda_0}P\right)\\ &+ 4i(\lambda_0 - \lambda_0^*)\partial_x P\left(1 - \frac{\lambda_0^* - \lambda_0}{\lambda - \lambda_0}P\right).\end{aligned}$$

The density matrix $\hat{\rho}$, containing the polarization variables and the level populations, must be formed from the terms which do not have poles, and are therefore given by the expression

$$\hat{\rho} = \rho_0 + 4i(\lambda_0 - \lambda_0^*)\partial_x P \tag{29}$$

Extracting the appropriate components leads to the expression in Eqs. (8c) to (8h).

Appendix B. **Single Soliton Solution for zero coherence.** From Eqs. (8c) to (8h) for the case of a pure imaginary soliton eigenvalue $\lambda_0 = i\beta$, and no initial coherence, $\mu_0 = 0$, we obtain the following expressions describing the material properties:

$$
\begin{aligned}
N &= \frac{2\big(|a|^2(1+\alpha) + |b|^2(1-\alpha)e^{\frac{\alpha x}{2\eta}}\big)}{\Big(e^{2\beta t - \frac{(1+\alpha)x}{8\beta}}(|a|^2 + |b|^2 e^{\frac{\alpha x}{2\beta}}) + e^{-2\beta t + \frac{(1+\alpha)x}{8\beta}}\Big)^2}, \\
n_+ &= \frac{1+\alpha}{2} - \frac{2|a|^2\big(1+\alpha+2|b|^2\alpha e^{4\beta t - \frac{(1-\alpha)x}{4\beta}}\big)}{\Big(e^{2\beta t - \frac{(1+\alpha)x}{8\beta}}(|a|^2 + |b|^2 e^{\frac{\alpha x}{2\beta}}) + e^{-2\beta t + \frac{(1+\alpha)x}{8\beta}}\Big)^2}, \\
n_- &= \frac{1-\alpha}{2} - \frac{2|b|^2\big((1-\alpha)e^{\frac{\alpha x}{2\beta}} - 2|a|^2\alpha e^{4\beta t - \frac{(1-\alpha)x}{4\beta}}\big)}{\Big(e^{2\beta t - \frac{(1+\alpha)x}{8\beta}}(|a|^2 + |b|^2 e^{\frac{\alpha x}{2\beta}}) + e^{-2\beta t + \frac{(1+\alpha)x}{8\beta}}\Big)^2}, \\
\mu &= \frac{-2ab^* e^{\frac{\alpha x}{4\beta}}\Big(e^{\frac{(1+\alpha)x}{4\beta}} + \alpha e^{4\beta t}(-|a|^2 + |b|^2 e^{\frac{\alpha x}{2\beta}})\Big)}{\Big(e^{-2\beta t + \frac{(1+\alpha)x}{4\beta}} + e^{2\beta t}(|a|^2 + |b|^2 e^{\frac{\alpha x}{2\beta}})\Big)^2}, \\
\rho_+ &= \frac{-a^* e^{2\beta t + \frac{(1+\alpha)x}{8\beta}}}{\Big(e^{\frac{(1+\alpha)x}{4\beta}} + e^{4\beta t}(|a|^2 + |b|^2 e^{\frac{\alpha x}{2\beta}})\Big)^2} \\
&\quad \times \Big((1+\alpha)e^{\frac{(1+\alpha)x}{4\beta}} + e^{4\beta t}(-|a|^2(1+\alpha) - |b|^2(1-3\alpha)e^{\frac{\alpha x}{2\beta}})\Big), \\
\rho_- &= \frac{-b^* e^{2\beta t + \frac{(1+\alpha)x}{8\beta}}}{\Big(e^{\frac{(1+\alpha)x}{4\beta}} + e^{4\beta t}(|a|^2 + |b|^2 e^{\frac{\alpha x}{2\beta}})\Big)^2} \\
&\quad \times \Big((1-\alpha)e^{\frac{(1+\alpha)x}{4\beta}} + e^{4\beta t}(-|a|^2(1+3\alpha) - |b|^2(1-\alpha)e^{\frac{\alpha x}{2\beta}})\Big).
\end{aligned}
$$

Appendix C. **Numerical Integration.** To numerically integrate the Maxwell-Bloch equations in (1) in the lab frame of reference, we use an implicit mid-point time integrator with the grid aligned to the characteristic speed (1 in this case). Discretizing space and time such that $x_j = j\Delta x$ and $t_n = n\Delta t$ with $\Delta x = \Delta t$ to align with the characteristics, the electric fields $E_j^n \approx E_+(x_j, t_n)$ and $F_j^n \approx E_-(x_j, t_n)$ are updated by

$$
\begin{aligned}
E_j^n &= E_{j-1}^{n-1} + \tfrac{\Delta t}{2}\left(R_{j-1}^{n-1} + R_j^n\right), && \text{(30a)} \\
F_j^n &= F_{j-1}^{n-1} + \tfrac{\Delta t}{2}\left(Q_{j-1}^{n-1} + Q_j^n\right), && \text{(30b)}
\end{aligned}
$$

for $j = 1 \ldots N$ and the boundary condition of a pulse entering is prescribed for E_0^n and F_0^n. No boundary condition is needed at $j = N$ since the characteristics exit the domian. The polarizations $R_j^n \approx \rho_+(x_j, t_n)$ and $Q_j^n \approx \rho_-(x_j, t_n)$ are updated

by

$$\begin{aligned}
R_j^n =& R_j^{n-1} + \frac{\Delta t}{4}\left(E_j^{n-1}(N_j^{n-1} - n_j^{n-1}) - F_j^{n-1}(\mu_j^{n-1})^*\right) \\
&+ \frac{\Delta t}{4}\left(E_j^n(N_j^n - n_j^n) - F_j^n(\mu_j^n)^*\right), \\
Q_j^n =& Q_j^{n-1} + \frac{\Delta t}{4}\left(F_j^{n-1}(N_j^{n-1} - m_j^{n-1}) - E_j^{n-1}\mu_j^{n-1}\right) \\
&+ \frac{\Delta t}{4}\left(F_j^n(N_j^n - m_j^n) - E_j^n\mu_j^n\right),
\end{aligned}$$

the populations $N_j^n \approx \mathcal{N}(x_j, t_n)$, $n_j^n \approx n_+(x_j, t_n)$ and $m_j^n \approx n_-(x_j, t_n)$ are updated by

$$\begin{aligned}
N_j^n =& N_j^{n-1} + \frac{\Delta t}{4}\left(E_j^{n-1}(R_j^{n-1})^* + (E_j^{n-1})^* R_j^{n-1}\right) \\
&+ \frac{\Delta t}{4}\left(F_j^{n-1}(Q_j^{n-1})^* + (F_j^{n-1})^* Q_j^{n-1}\right) \\
&+ \frac{\Delta t}{4}\left(E_j^n(R_j^n)^* + (E_j^n)^* R_j^n + F_j^n(Q_j^n)^* + (F_j^n)^* Q_j^n\right), \\
n_j^n =& n_j^{n-1} + \frac{\Delta t}{4}\left(E_j^{n-1}(R_j^{n-1})^* + (E_j^{n-1})^* R_j^{n-1}\right) \\
&+ \frac{\Delta t}{4}\left(E_j^n(R_j^n)^* + (E_j^n)^* R_j^n\right), \\
m_j^n =& m_j^{n-1} + \frac{\Delta t}{4}\left(F_j^{n-1}(Q_j^{n-1})^* + (F_j^{n-1})^* Q_j^{n-1}\right) \\
&+ \frac{\Delta t}{4}\left(F_j^n(Q_j^n)^* + (F_j^n)^* Q_j^n\right),
\end{aligned}$$

and the coherence $\mu_j^n \approx \mu(x_j, t_n)$ is updated by

$$\begin{aligned}
\mu_j^n =& \mu_j^{n-1} + \frac{\Delta t}{4}\left((E_j^{n-1})^* Q_j^{n-1} + F_j^{n-1}(R_j^{n-1})^*\right) \\
&+ \frac{\Delta t}{4}\left((E_j^n)^* Q_j^n + F_j^n(R_j^n)^*\right).
\end{aligned}$$

These implicit equations are iterated at each time-step until convergence is reached.

REFERENCES

[1] K. Shimoda, *Introduction to Laser Physics*, vol. 44 of *Springer Series on Optical Sciences* (Springer-Verlag, Berlin, 1986), second edition ed.

[2] P. N. Butcher and D. Cotter, *The Elements of Nonlinear Optics* (Cambridge University Press, Cambridge, 1990).

[3] R. W. Boyd, *Nonlinear Optics* (Academic Press, San Diego, Ca, 1992).

[4] A. C. Newell and J. V. Moloney, *Nonlinear Optics* (Addison-Wesley, 1992).

[5] L. Allen and J. H. Eberly, *Optical Resonance and Two-Level Atoms* (Dover, New York, 1987).

[6] M. J. Konopnicki and J. H. Eberly, "Simultaneous propagation of short different-wavelength optical pulses," Phys. Rev. A **24**, 2567–2583 (1981).

[7] M. J. Konopnicki, P. D. Drummond, and J. H. Eberly, "Theory of lossless propagation of simultaneous different-wavelength optical pulses," Opt. Commun. **36**, 313–316 (1981).

[8] A. Maimistov and A. M. Basharov, "Present state of self-induced transparency theory," Physics Reports-Review Section of Physics Letters **191**, 1–108 (1990).

[9] M. J. Ablowitz, D. J. Kaup, and A. C. Newell, "Coherent pulse propagation, a dispersive, irreversible phenomenon," Journal of Mathematical Physics **15**, 1852–1858 (1974).

[10] A. I. Maimistov and Y. M. Sklyarov, "The coherent interaction of light-pulses with a 3-level medium," Optika I Spektroskopiya **59**, 760–763 (1985).

[11] J. A. Byrne, I. R. Gabitov, and G. Kovačič, "Polarization switching of light interacting with a degenerate two-level optical medium," Phys. D **186**, 69–92 (2003).

[12] L. A. Bolshov, V. V. Likhanskii, and M. I. Persiantsev, "Contribution to the theory of coherent interaction of light pulses with resonant multilevel media," Sov. Phys. Jetp **57**, 524–528 (1983).
[13] A. M. Basharov and A. I. Maimistov, "Self-induced transparency when the resonance energy levels are degenerate," Sov. Phys. Jetp **60**, 913–919 (1984).
[14] A. I. Maimistov, "Rigorous theory of self-induced transparency in the case of a double resonance in a three-level medium," Sov. J. Quantum Electron. **14**, 385–389 (1984).
[15] V. Chernyak and V. Rupasov, "Polarization effects in self-induced transparency theory," Physics Letters A **108**, 434 – 436 (1985).
[16] G. Lamb, "Coherent-optical-pulse propagation as an inverse problem," Physical Review A **9**, 422–430 (1974).
[17] P. D. Lax, "Integrals of nonlinear equations of evolution and solitary waves," Commun. Pure and Appl. Math **21**, 467–490 (1968).
[18] I. Gabitov, V. Zakharov, and A. Mikhailov, "Maxwell-bloch equation and the inverse scattering method," Theor. Math. Phys. **63**, 328–343 (1985).
[19] S. Chakravarty, B. Prinari, and M. J. Ablowitz, "Inverse scattering transform for 3-level coupled maxwell-bloch equations with inhomogeneous broadening," Physica D **278–279**, 58–78 (2014).
[20] S. P. Novikov, S. V. Manakov, L. P. Pitaevskii, and V. E. Zakharov, *Theory of Solitons: The Inverse Scattering Method* (Plenum Press, New York, 1984).
[21] A. V. Rybin, "Application of the darboux transformation to inverse problems with variable spectral parameters," J. Phys. A: Math. Gen. **24**, 5235–5243 (1991).
[22] B. D. Clader, J. H. Eberly, "Two-pulse propagation in a partially phase-coherent medium," Phys. Rev. A **78**, 033803 (2008).
[23] E. P. Atkins, P. R. Kramer, G. Kovačič, and I. R. Gabitov, "Stochastic pulse switching in a degenerate resonant optical medium," Phys. Rev. A **85**, 043834 (2012).
[24] K. A. Newhall, E. P. Atkins, P. R. Kramer, G. Kovačič, and I. R. Gabitov, "Random polarization dynamics in a resonant optical medium," Optics Letters **38**, 893–895 (2013).
[25] L. J. Wang, A. Kuzmich, and A. Dogariu, "Gain-assisted superluminal light propagation," Nature **406**, 277–279 (2000).
[26] S. Li, G. Biondini, and G. Kovaγiγ, "Inverse-scattering transform for the Λ-configuration Maxwell-Bloch system with nonzero background," in preparation.

Received xxxx 20xx; revised xxxx 20xx.

E-mail address: knewhall@unc.edu
E-mail address: kovacg@rpi.edu
E-mail address: gabitov@math.arizona.edu